Journal of Organometallic Chemistry 696 (2011) 3223–3230

Contents lists available at ScienceDirect

Journal of Organometallic Chemistry

journal homepage: www.elsevier.com/locate/jorganchem

Synthesis, characterization and photophysical study of a series of neutral isocyano rhodium(I) complexes with pyridylindolide ligands

Wing-Kin Chu, Larry Tso-Lun Lo, Shek-Man Yiu, Chi-Chiu Ko*

Department of Biology and Chemistry, City University of Hong Kong, Tat Chee Avenue, Kowloon Tong, Hong Kong, China

ARTICLE INFO

Article history:
Received 30 March 2011
Received in revised form
22 June 2011
Accepted 28 June 2011

Keywords:
Rhodium
Isocyanide
Pyridylindole
Aggregation
Thermochromism

ABSTRACT

Pyridylindole ligand and its chloro substituted derivatives have been synthesized and incorporated into the square planar bis(phenylisocyano) rhodium(I) complexes to give a series of neutral rhodium(I) complexes with general formula of [Rh(**X-pyind**)(CNR)$_2$] (R = 2,6-(CH$_3$)$_2$-4-BrC$_6$H$_2$, 2,4-Cl$_2$-6-(CH$_3$O)C$_6$H$_2$, 2,4,6-Br$_3$C$_6$H$_2$, 2,4,6-Cl$_3$C$_6$H$_2$; L = 2-(2′-pyridyl)indole, 5-chloro-2-(2′-pyridyl)indole, 4,6-dichloro-2-(2′-pyridyl)indole). The structures of two complex precursors [Rh(cod)(**Cl-pyind**)] and [Rh(cod)(**Cl$_2$-pyind**)], and the target complex [Rh(**pyind**)(CNC$_6$H$_2$-2,4-Cl$_2$-6-(OCH$_3$))$_2$] were determined by X-ray crystallography. The UV–vis absorption properties of these complexes and their responses towards the change of temperature were also investigated.

1. Introduction

Cyclometalated transition metal complexes, such as those of phenylpyridine complexes, have attracted much attention in recent years as they are potentially useful in the development of the optical sensors and electroluminescent devices such as organic light-emitting diode (OLED) and light-emitting electrochemical cells (LEC) [1–5]. The enhanced luminescent behavior of these cyclometalated complexes is attributed to the strong ligand-field (LF) splitting resulting from the strong anionic σ-donating ligating atom, which raises common deactivating d-d LF state. On the other hand, the occurrence of close-lying, ligand-centered π–π* electronic transitions can allow facile tuning of emission wavelength across the whole visible spectrum. However, the study of these transition metal complex systems with cyclometalating ligands [6–8] have been mainly confined to metal centers, such as Ru(II) [9–11], Os(II) [12–14], Ir(III) [15–18] and Pt(II) [19–21], that are capable of undergoing cyclometalation as it requires the deprotonation of a C–H group. To retain the advantages of the cyclometalating ligands and to develop new classes of metal complexes with metal centers that are difficult to undergo cyclometalation, we propose to use other strong σ-donating and π-accepting bidentate anionic ligands with more acidic N-H proton such as substituted pyridylindolides (**X-pyind**) as the alternative to the cyclometalating N–C ligands. As an extension of our previous work in the development of tunable thermochromic bis(phenylisocyano) rhodium(I) diimine complexes with interesting thermally mediated aggregation [22], herein we report the synthesis and UV–vis absorption properties of a new series of neutral square planar bis(phenylisocyano) rhodium(I) complexes with different anionic cyclometalated pyridylindolide ligands. The thermochromism of these complexes have also been described.

2. Result and discussion

2.1. Synthesis and characterization

Using the method developed by Ugi et al. [23–26], all 2,4,6-trisubstituted phenylisocyanide ligands were synthesized by the dehydration of the corresponding N-phenyl formamide using phosphoryl chloride in the presence of triethylamine. All substituted pyridylindole ligands (**X-pyind**: **pyind**, **Cl-pyind**, **Cl$_2$pyind**) were prepared by the polyphosphoric acid (PPA) catalyzed Fischer indole synthesis from the corresponding substituted phenylhydrazones of the 2-acetylpyridine, which were freshly prepared from the condensation reactions between the substituted phenylhydrazium hydrochlorides and 2-acetylpyridine [27–30]. Reactions of [Rh(cod)Cl]$_2$ with the corresponding pyridylindole ligands in the presence of triethylamine in CH_2Cl_2 at room temperature gave the rhodium(I) complex precursors [Rh(cod)

* Corresponding author. Tel.: +852 3442 6958; fax: +852 3442 0522.
E-mail address: vinccko@cityu.edu.hk (C.-C. Ko).

0022-328X/$ – see front matter © 2011 Elsevier B.V. All rights reserved.
doi:10.1016/j.jorganchem.2011.06.032

(**X-pyind**)]. With the complex precursors, the bidentate 1,5-cyclooctadiene (cod) ligand could be readily replaced by substituted phenylisocyanide via the ligand substitution reactions with two mole equivalents of isocyanide ligands in THF solution at room temperature to afford the target complexes **1**–**10** [22,31,35]. After recrystallization from the slow diffusion of diethylether vapor into the concentrated dichloromethane or acetone solution of the complexes, analytically pure complexes isolated as yellow to yellowish green crystalline solids were obtained. The synthetic routes for the substituted pyridylindole ligands and the target complexes are summarized in Scheme 1.

All substituted pyridylindole ligands and their rhodium complexes **1**–**10** were characterized by elemental analyses, IR spectroscopy, ^{1}H NMR spectroscopy and positive FAB mass spectrometry. The crystal structures of two complex precursors, [Rh(cod)(**Cl-pyind**)] and [Rh(cod)(**Cl$_2$pyind**)], and **1** were also determined by X-ray crystallography. Upon coordination of the substituted pyridylindole ligands into rhodium complexes, most of the ^{1}H NMR signals of the ligands are upfield shifted compared to those of the free ligands and the corresponding indole NH NMR signal is not observed. This observation is in line with the increased electron density in the deprotonated anionic indolide moiety. The target complexes **1**–**10** show two strong C≡N stretches in the range of 2000–2130 cm^{-1}, consistent with *cis*- isocyanide arrangement in a square planar geometry. The lower stretching frequency of the C≡N stretches in these complexes compare to that of the free ligands can be attributed to a π back-bonding interaction between rhodium(I) metal center and isocyanide ligands through which C≡N bond of the isocyanide ligand is weaken due to the back-donation of electron density from the metal center to the anti-bonding π* orbital of the isocyanide ligands. The observation of the well-separated C≡N stretches with considerable different stretching frequencies is consistent with the significant difference in the electronic natures of the *trans*- neutral pyridine and anionic indolide moieties. This is in accordance with the longer C≡N distance and more bending of C≡N–C in the isocyanide ligand *trans*- to the indolide moiety in the crystal structure of **1**.

2.2. X-ray crystal structure determination

Single crystals of complexes [Rh(cod)(**Cl-pyind**)], [Rh(cod)(**Cl$_2$-pyind**)] and **1** were obtained by slow diffusion of diethylether vapor into a concentrated dichloromethane solution of the complexes. For the structure of [Rh(cod)(**Cl-pyind**)], there are two independent formula units in one crystallographic asymmetric unit. Perspective drawings of complexes [Rh(cod)(**Cl-pyind**)], [Rh(cod)(**Cl$_2$pyind**)] and **1** are depicted in Fig. 1. The structure determination data are collected in Table 1 and selected bond lengths and angles are summarized in Table 2. In these structures, the rhodium metal centers adopted distorted square planar geometry. The bite angles of the pyridylindolide ligands in these complexes are in the range of 78–80°, which are much smaller than the ideal angle 90° in a regular square planar geometry. The deviation from the ideal angle of 90° is a result of steric requirement of the chelating pyridylindolide ligand, which is typically observed in related cyclometalated transition metal complexes [1–5]. The noticeable shorter Rh–N(indole) bond distance than the Rh–N(pyridine) bond (averaged distance of 2.060 Å vs. 2.104 Å) is attributed to the stronger Coulombic interaction between the rhodium(I) cationic metal center and the anionic N-donor atoms and is commonly observed in other metal complexes with related ligands [32–36]. The shortest intermolecular Rh–Rh distances in these complexes are in the range of 6.02–8.10 Å, which are much longer than typical Rh–Rh distances (3.2–3.9 Å) in stacked Rh(I) complexes [22]. In the crystal structure of **1**, the rhodium metal center adopted a square planar geometry with the phenyl ring of the non-coplanar isocyanide ligand, which is *cis*- to the indolide moiety, tilted by 75° relative to the plane of the complexes. The highly tilted phenyl ring is attributed to the steric hindrance of phenyl moiety of the indole ring and the adjacent phenylisocyanide ligand. The Rh–C and C≡N bond lengths in complex **1** are in the range of 1.858–1.881 Å and 1.158–1.164 Å, respectively, similar to those reported in other related rhodium isocyanide complexes [37]. The deviations of the linearity of the isocyanide ligands in **1**, as reflected from the C≡N–C(phenyl) bond angles of 167.4° and 174.3° for two different isocyanide ligands, are the results of the π-back bonding interaction between the isocyanide ligands and the rhodium metal center [37–41]. The more bending observed for the isocyanide ligand *trans*- to the indolide moiety is suggestive of a better π-back bonding interaction. This is consistent with the stronger σ-donating and weaker π-accepting abilities of the anionic indolide moiety compared to those of the pyridine moiety.

2.3. Electronic absorption spectroscopy

The electronic absorption spectra of **1**–**10** in acetone show very intense absorption bands, with molar extinction coefficients in the order of 10^5 dm^3 mol^{-1} cm^{-1} in the UV region of 330–350 nm and moderately intense absorptions in the visible region of 380–480 nm (Table 3). With reference to the previous

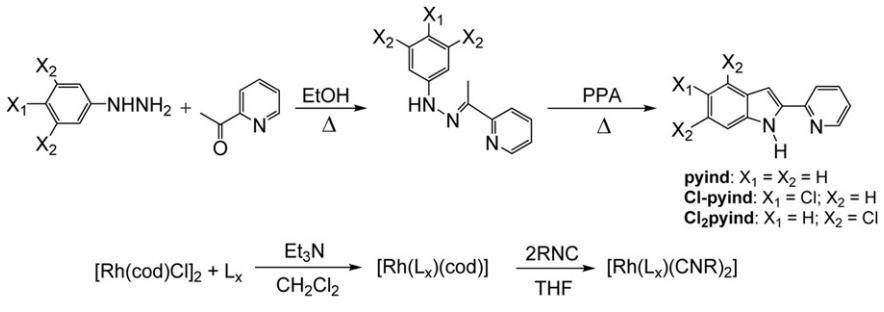

1: L_x =**prind**; R = 2,4-Cl_2-6-$(OCH_3)C_6H_2$
2: L_x = **pyind**; R = 2,4,6-$Br_3C_6H_2$
3: L_x = **pyind**; R = 2,4,6-$Cl_3C_6H_2$
4: L_x = **Cl-pyind**; R = 2,6-$(CH_3)_2$-4-BrC_6H_2
5: L_x = **Cl-pyind**; R = 2,4,6-$Br_3C_6H_2$
6: L_x = **Cl-pyind**; R = 2,4,6-$Cl_3C_6H_2$
7: L_x = **Cl$_2$pyind**; R = 2,6-$(CH_3)_2$-4-BrC_6H_2
8: L_x = **Cl$_2$pyind**; R = 2,4-Cl_2-6-$(OCH_3)C_6H_2$
9: L_x = **Cl$_2$pyind**; R = 2,4,6-$Br_3C_6H_2$
10: L_x = **Cl$_2$pyind**; R = 2,4,6-$Cl_3C_6H_2$

Scheme 1. Synthetic routes for substituted pyridylindole ligands and their isocyano rhodium(I) complexes

spectroscopic studies of the free isocyanide ligands and their transition metal complexes, these absorptions were tentatively assigned as spin allowed intraligand (IL) $\pi \rightarrow \pi^*$ transition of the isocyanide and pyridylindolide moieties. The two lowest energy absorptions at 380–430 nm and 440–480 nm are ascribed to the spin allowed and spin forbidden metal-to-ligand charge transfer (MLCT) [$d\pi(Rh) \rightarrow \pi^*(CNR)$] transitions, similar to those observed in other related tetra(phenylisocyano) Rh(I) complexes [42–45]. The peaks of these two absorptions are sensitive to the electronic nature of the isocyanide ligands. With the same pyridylindolide ligand, the absorption maxima of these bands are in line with the π-accepting ability of the isocyanide ligands (Fig. 2a):**2** (428, 478 nm) > **3** (415, 465 nm) > **1** (412, 462 nm) for complexes with **pyind**; **5** (417, 464 nm) > **6** (409, 461 nm) > **4** (384, 450 nm) for complexes with **Cl-pyind**; **9** (403, 460 nm) > **10** (398, 456 nm) > **8** (401, 454 nm) > **7** (384, 444 nm) for complexes with **Cl_2pyind**. These trends are in agreement with MLCT assignment. Besides, these absorption bands also show dependence on the electronic nature of the pyridylindolide ligand. For complexes with the same isocyanide ligands, the absorption energies of these bands are higher for the complex with pyridylindolide ligand bearing more electron withdrawing substituents (**Cl_2pyind** > **Cl-pyind** > **pyind**) as reflected by the order of λ_{abs}: **9** (403, 460 nm) < **5** (417, 464 nm) < **2** (428, 478 nm) and **10** (398, 456 nm) < **6** (409, 461 nm) < **3** (415, 465 nm) (Fig. 2b). This energy trend can be attributed to the better stabilization of the dπ(Rh) orbital as a result of the more electron withdrawing substituents in the pyridylindolide ligand, leading to a higher energy of MLCT [$d\pi(Rh) \rightarrow \pi^*(CNR)$] transition.

As demonstrated in our previous communication [22], all the square planar bis(phenylisocyano) rhodium(I) diimine complexes with general formula of $[Rh(N{-}N)(CNR)_2]BF_4$ (N–N = bpy, Me_2bpy, Br_2phen; CNR = $CNC_6H_3(CH_3)$-2,6, $CNC_6H_2Br_3$-2,4,6, CNC_6H_4Cl-4) were found to show thermochromic behavior due to the thermally mediated aggregation properties. The thermal responses of complexes **1** – **10** in THF solutions were also studied by the UV–vis absorption spectroscopy. However, unlike the bis(phenylisocyano) rhodium(I) diimine complexes, in which the thermochromic behavior for all the solutions of the complexes with different substituents of diverse electronic and steric natures could be readily observed at low concentration, only the solutions of **3**, **6** and **10** all with the 2,4,6-trichlorophenylisocyanide ligand at concentration

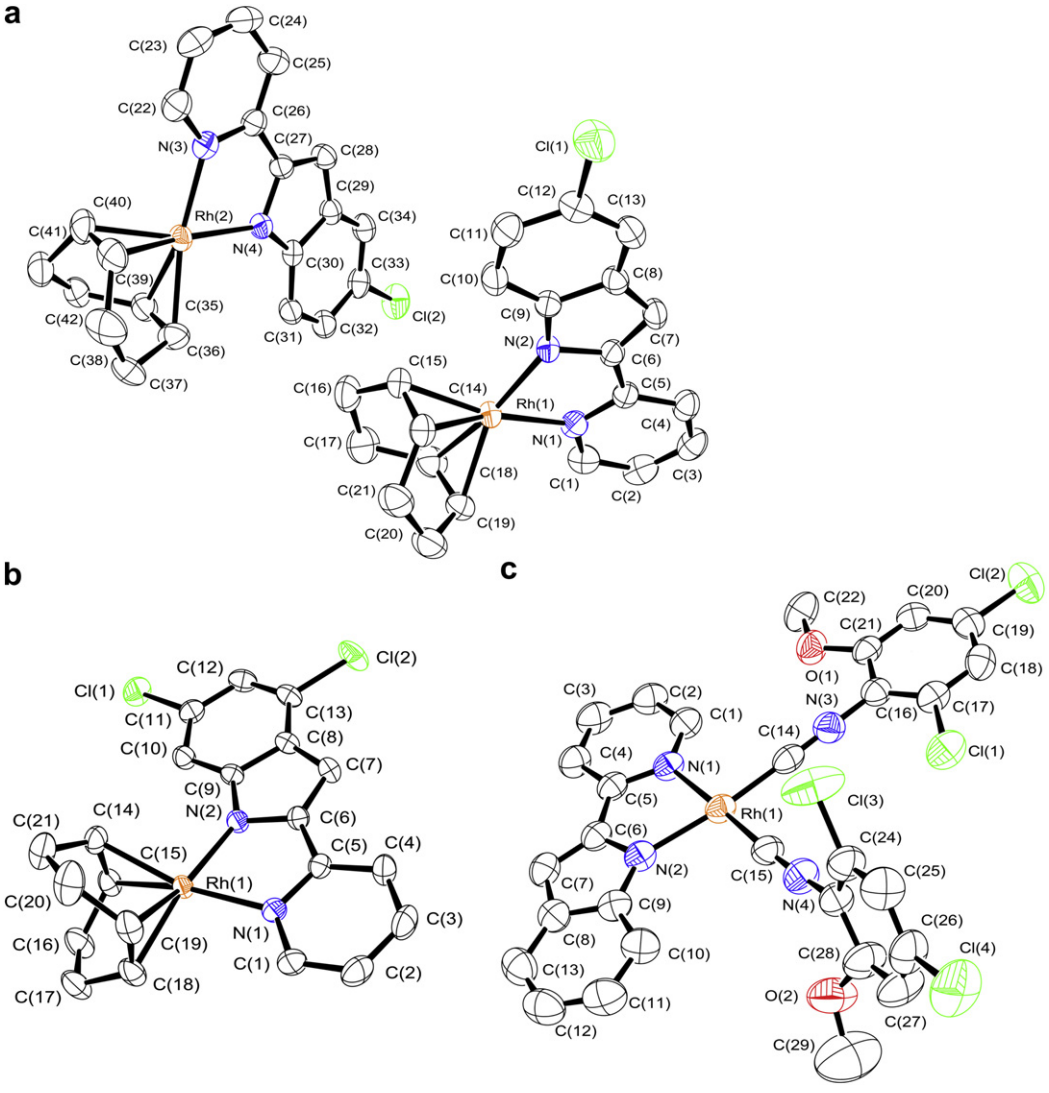

Fig. 1. Perspective drawings of (a) two independent molecules of [Rh(cod)(**Cl-pyind**)], (b) [Rh(cod)(**Cl_2pyind**)] and (c) **1** with atom numbering. Hydrogen atoms have been omitted for clarity. Thermal ellipsoids are shown at the 50% probability level.

Table 1
Crystal and structure determination data for [Rh(cod)(**Cl-pyind**)], [Rh(cod)(**Cl$_2$pyind**)] and **1**.

	[Rh(cod)(**Cl-pyind**)]	[Rh(cod)(**Cl$_2$pyind**)]	**1**
Formula	$C_{21}H_{20}ClN_2Rh$	$C_{21}H_{19}Cl_2N_2Rh$	$C_{29}H_{19}Cl_4N_4O_2Rh$
M_r	438.75	473.19	700.19
T (K)	293(2)	293(2)	293(2)
a (Å)	11.05083(13)	7.74390(10)	34.1908(8)
b (Å)	13.15739(18)	10.44030(10)	8.09680(10)
c (Å)	13.28968(19)	11.82230(10)	24.0801(6)
α (°)	110.0538(13)	77.2380(10)	90
β (°)	93.8999(11)	80.1270(10)	121.211(3)
γ (°)	105.9273(11)	75.6790(10)	90
V (Å^3)	1717.14(4)	896.308(16)	5071.4(2)
Crystal color	Orange	Yellow	Red
Crystal system	Triclinic	Triclinic	Monoclinic
Space group	Pī	Pī	C2/c
Z	4	2	8
F(000)	888	476	2800
D_c (g cm^{-3})	1.697	1.753	1.631
Crystal dimensions, (mm)	0.7 × 0.3 × 0.3	0.5 × 0.3 × 0.1	0.5 × 0.3 × 0.2
λ (Å) (graphite-monochromated, Mo-K$_\alpha$)	0.71073	0.71073	0.71073
μ (mm^{-1})	1.16	1.26	1.01
Collection range	$3.5° \le \theta \le 25.0°$ (h: −13 to 13; k: −15 to 15; l: −15 to 15)	$3.4° \le \theta \le 25.0°$ (h: −9 to 9; k: −12 to 12; l: −14 to 14)	$3.5° \le \theta \le 25.0°$ (h: −40 to 40; k: −9 to 9; l: −28 to 28)
Completeness to theta	99.6%	99.7%	99.7%
No. of data collected	31092	19727	23747
No. of unique data	6018	3158	5009
No. of data used in refinement, m	5498	3096	4304
No. of parameters refined, p	478	235	380
R[a]	0.020	0.018	0.024
wR[a]	0.053	0.050	0.060
Goodness-of-fit, S	1.10	1.15	1.03
Maximum shift $(\Delta/\sigma)_{max}$	0.004	0.001	0.003
Residual extrema in final difference map, eÅ^{-3}	+0.31, −0.54	+0.34, −0.59	+0.35, −0.33

[a] $w = 1/[\sigma^2(F_o^2) + (aP)^2 + bP]$, where P is $[2F_c^2 + \mathrm{Max}(F_o^2, 0)]/3$.

> 0.35 mM exhibit observable thermochromism (Fig. 3). This suggests that the aggregation affinity of these complexes is much lower than that of the diimine analogous complexes. The lower aggregation affinity of these complexes may be explained by the increased steric repulsion as the phenyl ring of the non-coplanar isocyanide ligand is considerably more deviated from the planarity of complexes due to the more sterically demanding indole ring in the pyridylindolide ligand. While the absence of the thermochromic behavior of other complexes (**1**–**2**, **4**–**5** and **7**–**9**) may be attributed to the more sterically demanding nature of their isocyanide ligands compared to the 2,4,6-trichlorophenylisocyanide ligand.

Upon cooling, the solutions of **3**, **6** and **10** gradually change their color from yellow to green with the evolution of a new absorption band at *ca*. 563–607 nm. This new absorption band grows in intensity and shows a slight red shift as temperature decreases. In light of previous spectroscopic and aggregation studies on rhodium(I) complexes with isocyanide ligands [22,41,44,46,47], this absorption is tentatively assigned to the transition from $d\sigma^*[d_z^{2*}(Rh)]$ to $p\sigma[p_z(Rh)]$ of the dimeric complex [Rh(**X-pyind**)($CNC_6H_2Cl_3$-2,4,6)$_2$]$_2$ (Scheme 2). The slight red shift of the new absorption (Fig. 3a) may be ascribed to the shortening of the Rh-Rh distance in the dimeric units as the temperature decreases. As stronger Rh-Rh interaction would raise the $d\sigma^*[d_z^{2*}(Rh)]$ orbital and stabilize $p\sigma[p_z(Rh)]$, both factors would also lead to narrowing down of the energy gap of $d\sigma^*[d_z^{2*}(Rh)]$ to $p\sigma[p_z(Rh)]$ transition. On warming to the room temperature, the new absorption decreases in intensity and the absorption spectra reverts back into its original spectra before cooling.

Table 2
Selected bond lengths [Å] and angles [°] with estimated standard deviations in parenthese for [Rh(cod)(**Cl-pyind**)], [Rh(cod)(**Cl$_2$pyind**)] and **1**.

[Rh(cod) (**Cl-pyind**)]	Rh(1)–N(1)	2.108(16)	Rh(1)–N(2)	2.063(16)
	Rh(2)–N(3)	2.114(17)	Rh(2)–N(4)	2.072(16)
	N(1)–Rh(1)–N(2)	79.69(6)	N(3)–Rh(2)–N(4)	79.39(6)
[Rh(cod) (**Cl$_2$pyind**)]	Rh(1)–N(1)	2.104(15)	Rh(1)–N(2)	2.060(15)
	N(1)–Rh(1)–N(2)	79.46(6)		
1	Rh(1)–N(1)	2.095(17)	Rh(1)–N(2)	2.052(18)
	Rh(1)–C(14)	1.881(3)	Rh(1)–C(15)	1.858(2)
	N(3)–C(14)	1.158(3)	N(4)–C(15)	1.164(3)
	N(1)–Rh(1)–N(2)	78.99(7)	C(14)–Rh(1)–C(15)	87.00(9)
	N(1)–Rh(1)–C(14)	94.57(8)	N(2)–Rh(1)–C(15)	99.47(8)
	C(14)–N(3)–C(16)	174.3(2)	C(15)–N(4)–C(23)	167.4(3)

3. Conclusion

A new class of square planar bis(phenylisocyano) pyridylindolido rhodium(I) complexes, [Rh(**X-pyind**)(CNR)$_2$], with

Table 3
Photophysical data for complexes **1**–**10**.

Complex	T/K	Absorption[a] λ_{abs}/nm (ε/dm^{3}mol^{-1}cm^{-1})
1	298	348 (38755), 412 (13945), 462 sh (6390)
2	298	344 (24010), 428 (10585), 478 sh (2910)
3	298	344 (27880), 415 (11645), 465 sh (3710)
	173	579[b]
4	298	345 (28055), 384 (13385), 450 sh (3820)
5	298	344 (33775), 417 (15005), 464 sh (5025)
6	298	340 (30515), 409 (8755), 461 sh (2910)
	173	607[b]
7	298	330 (29140), 384 (15680), 444 sh (3700)
8	298	344 (24210), 401 (10110), 454 sh (2295)
9	298	341 (33325), 403 (17590), 460 sh (3060)
10	298	344 (10570), 398 (6625), 456 sh (1080)
	173	563[b]

[a] In acetone.
[b] Absorption of the dimeric unit of the complexes in THF.

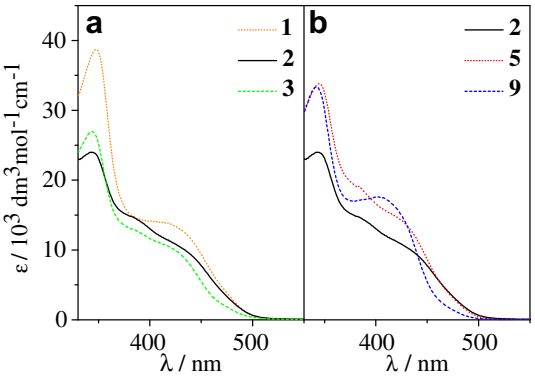

Fig. 2. Overlaid UV–vis spectra of (a) **1**, **2**, **3** and (b) **2**, **5**, **9** in acetone solutions at 298 K.

isocyanide and pyridylindolide ligands of different electronic and steric features has been successfully synthesized. These complexes have been characterized by ^{1}H NMR and IR spectroscopy, mass spectrometry and elemental analyses. The X-ray crystal structures of two of the complex precursors [Rh(cod)(**Cl-pyind**)] and [Rh(cod)(**Cl$_2$pyind**)], and the target complex [Rh(**pyind**)($CNC_6H_2Cl_2$-2,4-OCH_3-6)$_2$] have also been determined. The UV–vis absorption properties of these complexes and responses towards the change of the temperature have been investigated. Of all complexes investigated, only the solutions of **3**, **6** and **10** all with the 2,4,6-trichlorophenylisocyanide ligand exhibit observable thermochromism.

4. Experimental

4.1. Materials and reagents

Phenylhydrazine hydrochloride and ortho-phosphoric acid were purchased from Merck Chemical Company. 4-Chlorophenylhydrazinum hydrochloride and 3,5-chlorophenylhydrazinum hydrochloride were obtained from Meryer Chemical Company. 2-Acetylpyridine, 2,4,6-tribromoaniline, 2,4,6-trichloroaniline, 4-bromo-2,6-dimethylaniline, 1,5-cyclooctadiene (cod), formic acid, phosphoryl chloride, phosphorus pentoxide and triethylamine were obtained from Aldrich Chemical Company and used as received. Rhodium(III) chloride hydrate was obtained from Strem Chemical Inc. [Rh(cod)Cl]$_2$ was synthesized from the reaction between rhodium(III) chloride and cod according to a literature procedure [22,35]. Substituted phenylisocyanide ligands, $CNC_6H_2(CH_3)_2$-2,6-Br-4, $CNC_6H_2Cl_2$-2,4-OCH_3-6, $CNC_6H_2Br_3$-2,4,6, $CNC_6H_2Cl_3$-2,4,6 were prepared from the corresponding substituted formamides according to the synthetic methodology reported by Ugi et al. [23–26]. All other reagents and solvents were of analytical grade and were used as received.

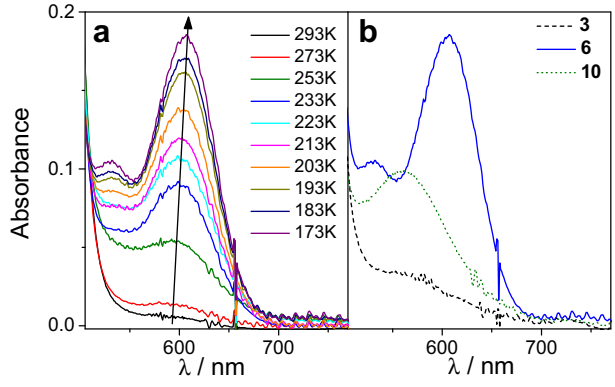

Fig. 3. (a) The absorption spectral changes of **6** (0.39 mM) in THF solution upon cooling from 293 K to 173 K. (b) The overlaid absorption spectra of **3**, **6** and **10** at the concentration of 0.39 mM in THF solution at 173 K.

4.2. Physical measurements and instrumentation

^{1}H NMR spectra were recorded on a Bruker AV400 (400 MHz) FT-NMR spectrometer at 293 K. Chemical shifts (δ, ppm) were reported relative to tetramethylsilane (Me_4Si). Infrared spectra of the solid samples as KBr discs were obtained in the range of 4000–400 cm^{-1} using an AVATAR 360 FTIR spectrometer. All positive-ion FAB mass spectra were recorded on a Finnigan MAT95 mass spectrometer. The elemental analyses were performed on an Elementar Vario EL III Analyser. Electronic absorption spectra were recorded on a Hewlett-Packard 8453 or Hewlett-Packard 8452A diode array spectrophotometer with the temperature control using an Oxford Instruments cryostat (Optistat DN).

4.3. X-ray crystal structure determination

The crystal structures were determined on an Oxford Diffraction Gemini S Ultra X-ray single crystal diffractometer using graphite monochromatised Mo-K_α radiation ($\lambda = 0.71073$ Å). The structures were solved by direct methods employing SHELXL-97 program [48] on PC. Rh and many non-H atoms were located according to the direct methods. The positions of other non-hydrogen atoms were found after successful refinement by full-matrix least-squares using SHELXL-97 program [48] on a PC. In the final stage of least-squares refinement, all non-hydrogen atoms were refined anisotropically. H atoms were generated by program SHELXL-97 [48]. The positions of H atoms were calculated based on riding mode with thermal parameters equal to 1.2 times that of the associated C atoms, and participated in the calculation of final *R*-indices. A conventional index R_1 based on observed *F* values larger than $4\sigma(F_o)$ is given (corresponding to Intensity $\geq 2\sigma(I)$). $wR_2 = \{\Sigma[w(F_o^2 - F_c^2)^2]/\Sigma[w(F_o^2)^2]\}^{1/2}$, $R_1 = \Sigma||F_o| - |F_c||/\Sigma|F_o|$, The Goodness of Fit is always based on F^2: $\mathrm{GooF} = S = \{\Sigma[w(F_o^2 - F_c^2)^2]/(n-p)\}^{1/2}$, where *n* is the number of reflections and *p* is the total number of parameters refined. The weighting scheme is: $w = 1/[\sigma^2(F_o^2) + (\alpha P)^2 + bP]$, where *P* is $[2F_c^2 + \mathrm{Max}(F_o^2, 0)]/3$.

4.4. Synthesis

Unless otherwise specified, all the syntheses were performed under strictly anaerobic and anhydrous conditions in an inert atmosphere of argon using standard Schlenk techniques.

4.4.1. Synthesis of substituted 2-acetylpyridine phenylhydrazones

4.4.1.1. General synthetic procedure: These compounds were synthesized according to a modified literature procedure [27–30]. A solution of 2-acetylpyridine (1 g, 8.0 mmol) and the corresponding substituted phenylhydrazium hydrochloride (1 mol equiv.) in EtOH (20 mL) were heated to reflux for 30 min. After that, the mixture was cooled to room temperature to commence precipitation. The precipitate was collected by suction filtration and washed with cold ethanol. After vacuum drying, the substituted 2-acetylpyridine phenylhydrazones were obtained as orange powder, which were sufficiently pure for the use in the syntheses of the corresponding substituted 2-(2′-pyridyl)indoles. Yield: 75–80%.

*4.4.2. 2-(2′-Pyridyl)indole (**pyind**)*

The ligand was synthesized according a literature procedure commonly employed for Fischer indole synthesis [27–30]. To a mixture of 2-acetylpyridine phenylhydrazone (2 g, 9.4 mmol) and polyphosphoric acid (10 g) was heated to reflux for 1.5 h. After cooling to room temperature, the resulting mixture was neutralized by 10% NaOH aqueous solution and then extracted with CH_2Cl_2 (3×50 mL). The combined organic extracts was washed with deionized water and dried over $MgSO_4$. After removal of the solvent under reduced pressure, the crude product was further purified by column chromatography on silica gel using CH_2Cl_2 as eluent. Subsequent recrystallization by slow diffusion of diethylether vapor into a concentrated acetone solution of the compound gave the analytically pure **pyind** as off-white powder. Yield: 19.6% (0.36 g, 1.8 mmol); ^{1}H NMR (400 MHz, $CDCl_3$, 298 K): δ 7.02 (dd, 1H, $J = 2.0$, 0.9 Hz, 3-indolinyl H's), 7.12 (td, 1H, $J = 8.0$, 0.9 Hz, 5-indolinyl H's), 7.18 (ddd, 1H, $J = 8.0$, 4.9, 1.2 Hz, 5′-pyridyl H's), 7.21 (td, 1H, $J = 8.0$, 1.2 Hz, 6-indolinyl H's), 7.41 (dd, 1H, $J = 8.0$, 0.9 Hz, 7-indolinyl H's), 7.67 (dd, 1H, $J = 8.0$, 0.9 Hz, 4-indolinyl H's), 7.72 (td, 1H, $J = 8.0$, 1.7 Hz, 4′-pyridyl H's), 7.80 (ddd, 1H, $J = 8.0$, 1.2, 1.0 Hz, 3′-pyridyl H's), 8.58 (ddd, 1H, $J = 4.9$, 1.7, 1.0 Hz, 6′-pyridyl H's), 9.59 (s, 1H, 1-indolinyl H's); positive-ion FAB-MS: m/z 195.1 $[M]^+$.

*4.4.3. 5-Chloro-2-(2′-pyridyl)indole (**Cl-pyind**)*

The ligand was synthesized according to a procedure similar to that of **pyind** except 2-acetylpyridine-4′-chlorophenylhydrazone (3 g, 12 mmol) was used in place of 2-acetylpyridine phenylhydrazone. After recrystallization by slow diffusion of diethylether vapor into a concentrated acetone solution of the ligand, **Cl-pyind** was obtained as colorless needle-shaped crystals. Yield: 11.6% (0.32 g, 1.4 mmol); ^{1}H NMR (400 MHz, $CDCl_3$, 298 K): δ 6.95 (d, 1H, $J = 2.1$ Hz, 3-indolinyl H's), 7.15–7.21 (m, 2H, 6-indolinyl H's, 5′-pyridyl H's), 7.32 (d, 1H, $J = 8.7$ Hz, 7-indolinyl H's), 7.61 (d, 1H, 1.2 Hz, 4-indolinyl H's), 7.73 (td, 1H, $J = 8.7$, 1.7 Hz, 4′-pyridyl H's), 7.80 (ddd, 1H, $J = 8.0$, 1.2, 1.0 Hz, 3′-pyridyl H's), 8.58 (ddd, 1H, $J = 4.9$, 1.7, 1.0 Hz, 6′-pyridyl H's), 9.60 (s, 1H, 1-indolinyl H's); Positive-ion FAB-MS: m/z 229.0 $[M]^+$; Elemental analyses calcd (%) for **Cl-pyind**: C 68.28, H 3.97, N 12.25; found: C 68.05, H 4.01, N 12.26.

*4.4.4. 4,6-Dichloro-2-(2′-pyridyl)indole (**Cl$_2$pyind**)*

The ligand was synthesized by a procedure similar to that of **pyind** except 2-acetylpyridine-3′,5′-dichlorophenylhydrazone (3 g, 10.6 mmol) was used in place of 2-acetylpyridine phenylhydrazone. After recrystallization by slow diffusion of diethylether vapor into a concentrated acetone solution of the ligand, **Cl$_2$pyind** was obtained as colorless needle-shaped crystals. Yield: 19.4% (0.54 g, 2.0 mmol); ^{1}H NMR (400 MHz, $CDCl_3$, 298 K): δ 7.06 (dd, 1H, $J = 2.1$, 0.9 Hz, 3-indolinyl H's), 7.13 (d, 1H, $J = 1.6$ Hz, 5-indolinyl H's), 7.24 (ddd, 1H, $J = 7.9$, 4.9, 1.2 Hz, 5′-pyridyl H's), 7.27 (dd, 1H, $J = 1.6$, 0.9 Hz, 7-indolinyl H's), 7.75 (td, 1H, $J = 7.9$, 1.7 Hz, 4′-pyridyl H's), 7.83 (ddd, 1H, $J = 7.9$, 1.2, 1.0 Hz, 3′-pyridyl H's), 8.58 (ddd, 1H, $J = 4.9$, 1.7, 1.0 Hz, 6′-pyridyl H's), 9.87 (s, 1H, 1-indolinyl H's); Positive-ion FAB-MS: m/z 263.0 $[M]^+$; Elemental analyses calcd (%) for **Cl$_2$pyind**: C 59.34, H 3.06, N 10.65; found: C 59.09, H 3.13, N 10.67.

*4.4.5. Synthesis of precursor complexes [Rh(cod)(**X-pyind**)]*

General synthetic procedure: To a solution of $[Rh(cod)Cl]_2$ (100 mg, 0.203 mmol) and pyridylindole ligand (2 mol equiv.) in CH_2Cl_2 (50 mL) was added, triethylamine (3 mol equiv.). The resulting solution was then stirred at room temperature for 24 h. Thereafter, the resulting solution was washed with deionized water. Recrystallization by the slow diffusion of diethylether vapor into a concentrated dichloromethane solution of the complexes gave desired precursor complexes [Rh(cod)(**X-pyind**)] as analytically pure products.

*4.4.5.1. [Rh(cod)(**pyind**)]* Yield: 97.1% (160 mg, 0.39 mmol); ^{1}H NMR (400 MHz, $CDCl_3$, 298 K): $\delta = 1.93$–2.12 (m, 4H, CH_2 of cod), 2.47–2.61 (m, 4H, CH_2 of cod), 4.01 (s, 2H, CH of cod), 5.53 (s, 2H, CH of cod), 6.87–7.02 (m, 5H, 3,5,6,7-indolinyl H's, 5′-pyridyl H's), 7.46 (d, 1H, $J = 5.6$ Hz, 4-indolinyl H's), 7.53 (d, 1H, $J = 7.7$ Hz, 4′-pyridyl H's), 7.64 (td, 1H, $J = 7.7$, 1.4 Hz, 3′-pyridyl H's), 7.73 (d, 1H, $J = 7.7$ Hz, 6′-pyridyl H's).

*4.4.5.2. [Rh(cod)(**Cl-pyind**)]* Yield: 55.8% (100 mg, 0.23 mmol); ^{1}H NMR (400 MHz, $CDCl_3$, 298 K): δ 1.94–2.11 (m, 4H, CH_2 of cod), 2.48–2.61 (m, 4H, CH_2 of cod), 4.04 (d, 2H, $J = 2.5$ Hz, CH of cod), 5.45 (d, 2H, $J = 2.5$ Hz, CH of cod), 6.83 (s, 1H, 3-indolinyl H's), 6.86 (d, 1H, $J = 8.9$ Hz, 6-indolinyl H's), 6.90 (dd, 1H, $J = 8.9$, 2.0 Hz, 7-indolinyl H's), 7.00 (td, 1H, $J = 7.1$, 1.4 Hz, 5′-pyridyl H's), 7.47–7.52 (m, 2H, 4-indolinyl H's, 4′-pyridyl H's), 7.66 (td, 1H, $J = 7.1$, 1.4 Hz, 3′-pyridyl H's), 7.71 (d, 1H, $J = 7.1$ Hz, 6′-pyridyl H's); Elemental analyses Calcd (%) for [Rh(cod)(**Cl-pyind**)]: C 58.92, H 5.59, N 5.98; found: C 58.64, H 5.29, N 6.21.

*4.4.5.3. [Rh(cod)(**Cl$_2$pyind**)]* Yield: 76.4% (148 mg, 0.31 mmol); ^{1}H NMR (400 MHz, $CDCl_3$, 298 K): δ 1.97–2.11 (m, 4H, CH_2 of cod), 2.52–2.57 (m, 4H, CH_2 of cod), 4.07 (s, 2H, CH of cod), 5.41 (s, 2H, CH of cod), 6.83 (s, 1H, 3-indolinyl H's), 6.91 (s, 1H, 5-indolinyl H's), 6.96 (s, 1H, 7-indolinyl H's), 7.03 (t, 1H, $J = 6.8$ Hz, 5′-pyridyl H's), 7.49 (d, 1H, $J = 6.8$ Hz, 4′-pyridyl H's), 7.70 (d, 1H, $J = 6.8$ Hz, 3′-pyridyl H's), 7.76 (d, 1H, $J = 6.8$ Hz, 6′-pyridyl H's). Elemental analyses Calcd (%) for [Rh(cod)(**Cl$_2$pyind**)]·½CH_2Cl_2: C 51.74, H 4.80, N 5.13; found (%): C 51.54, H 4.54, N 5.39.

*4.4.6. Synthesis of [Rh(**X-pyind**)(CNR)$_2$]*

General synthetic procedure: To a solution of [Rh(cod)(**X-pyind**)] (0.12 mmol) in THF (40 mL) was added in a dropwise manner,

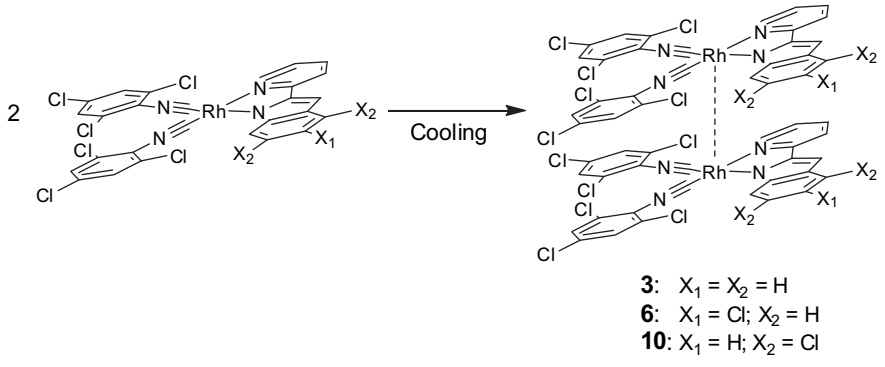

Scheme 2. Thermally mediated dimerization of **3**, **6** and **10**

a solution of substituted phenylisocyanide ligand (2 mol equiv.) in THF (10 mL). The resulting mixture was stirred at room temperature for 24 h. Thereafter, the solvent was removed under reduced pressure and the crude product was washed with n-pentane (3 × 10 mL). The crude product was further purified by recrystallization to give the analytically pure complex.

*4.4.6.1. [Rh(**pyind**)(CNC$_6$H$_2$Cl$_2$-2,4-OCH$_3$-6)$_2$] (**1**)* After recrystallization by the slow diffusion of diethylether vapor into a concentrated dichloromethane solution of **1**, analytically pure complex was obtained as yellow crystalline solids. Yield: 34.7%; ^{1}H NMR (400 MHz, $CDCl_3$, 298 K): δ 3.91 (s, 3H, $-OCH_3$), 3.94 (s, 3H, $-OCH_3$), 6.86 (d, 1H, 2.0 Hz, 3-indolinyl H's), 6.87–6.92 (m, 2H, phenyl H's), 6.93–7.02 (m, 3H, 5′-pyridyl H's, 5,6-indolinyl H's), 7.06–7.10 (m, 2H, phenyl H's), 7.55 (d, 1H, J = 7.8 Hz, 7-indolinyl H's), 7.68 (td, 1H, J = 8.0, 1.5 Hz, 4-indolinyl H's), 7.76 (d, 1H, J = 8.0 Hz, 4′-pyridyl H's), 7.96 (d, 1H, J = 8.0 Hz, 3′-pyridyl H's), 8.82 (d, 1H, J = 5.8 Hz, 6′-pyridyl H's); Positive-ion FAB-MS: m/z 699.9 $[M]^+$; IR (KBr disc, ν/cm^{-1}): 2122, 2049 ν(N≡C); Elemental analyses Calcd (%) for **1**: C 49.74, H 2.74, N 8.00; found (%): C 49.64, H 2.89, N 8.02.

*4.4.6.2. [Rh(**pyind**)(CNC$_6$H$_2$Br$_3$-2,4,6)$_2$] (**2**)* After recrystallization by the slow diffusion of diethylether vapor into a concentrated acetone solution of **2**, analytically pure complex was obtained as yellow crystalline solids. Yield: 35.8%; ^{1}H NMR (400 MHz, $CDCl_3$, 298 K): δ 6.90 (s, 1H, 3-indolinyl H's), 6.97–7.04 (m, 3H, 5′-pyridyl H's, 5,6-indolinyl H's), 7.55 (d, 1H, J = 7.0 Hz, 7-indolinyl H's), 7.70 (t, 1H, J = 8.0 Hz, 4-indolinyl H's), 7.75–7.78 (m, 3H, 4′-pyridyl H's, phenyl H's), 7.80 (m, 2H, phenyl H's), 7.85 (d, 1H, 8.0 Hz, 3′-pyridyl H's), 8.84 (d, 1H, J = 5.5 Hz, 6′-pyridyl H's). Positive-ion FAB-MS: m/z 975.5 $[M]^+$; IR (KBr disc, ν/cm^{-1}): 2104, 2008 ν(N≡C); Elemental analyses Calcd (%) for **2**·$CH_3CH_2OCH_2CH_3$: C 35.46, H 2.11, N 5.34; found: C 35.77, H 2.11, N 5.26.

*4.4.6.3. [Rh(**pyind**)(CNC$_6$H$_2$Cl$_3$-2,4,6)$_2$] (**3**)* After recrystallization by the slow diffusion of diethylether vapor into a concentrated dichloromethane solution of **3**, analytically pure complex was obtained as yellow crystalline solids. Yield: 37.7%; ^{1}H NMR (400 MHz, $CDCl_3$, 298 K): δ 6.90 (s, 1H, 3-indolinyl H's), 6.94 (dd, 1H, J = 8.8, 2.1 Hz, 5-indolinyl H's), 7.0–7.04 (m, 2H, 5′-pyridyl H's, 6-indolinyl H's), 7.42 (s, 2H, phenyl H's), 7.46 (s, 2H, phenyl H's), 7.50 (d, 1H, 2.1 Hz, 7-indolinyl H's), 7.71–7.78 (m, 3H, 3′,4′-pyridyl H's, 4-indolinyl H's), 8.77 (dd, 1H, 5.6, 1.0 Hz, 6′-pyridyl H's); Positive-ion FAB-MS: m/z 709.1 $[M]^+$; IR (KBr disc, ν/cm^{-1}): 2115, 2027 ν(N≡C); Elemental analyses Calcd (%) for **3**·0.5CH_2Cl_2: C 43.95, H 1.88, N 7.46; found: C 43.84, H 1.86, N 7.51.

*4.4.6.4. [Rh(**Cl-pyind**)(CNC$_6$H$_2$Br-4-(CH$_3$)$_2$-2,6)$_2$] (**4**)* After recrystallization by the slow diffusion of diethylether vapor into a concentrated dichloromethane solution of **4**, analytically pure complex was obtained as yellow crystalline solids. Yield: 46.9%; ^{1}H NMR (400 MHz, $CDCl_3$, 298 K): δ 2.44 (s, 6H, $-CH_3$), 2.49 (s, 6H, $-CH_3$), 6.87 (dd, 1H, J = 7.8, 2.1 Hz, 6-indolinyl H's), 6.91 (s, 1H, 3-indolinyl H's), 6.99 (ddd, 1H, J = 7.2, 5.6, 1.5 Hz, 5′-pyridyl H's), 7.28 (s, 2H, phenyl H's), 7.30 (s, 2H, phenyl H's), 7.51–7.55 (m, 2H, 4,7-indolinyl H's), 7.73 (dd, 1H, J = 7.2, 1.5 Hz, 4′-pyridyl H's), 7.77 (d, 1H, J = 7.2, 1.5 Hz, 3′-pyridyl H's), 8.61 (d, 1H, 5.6 Hz, 6′-pyridyl H's); Positive-ion FAB-MS: m/z 749.9 $[M]^+$; IR (KBr disc, ν/cm^{-1}): 2111, 2056 ν(N≡C); Elemental analyses Calcd (%) for **4**: C 49.60, H 3.22, N 7.46; found: C 49.58, H 3.39, N 7.43.

*4.4.6.5. [Rh(**Cl-pyind**)(CNC$_6$H$_2$Br$_3$-2,4,6)$_2$] (**5**)* After recrystallization by the slow diffusion of diethylether vapor into a concentrated dichloromethane solution of **5**, analytically pure complex was obtained as yellow crystalline solids. Yield: 37.5%; ^{1}H NMR (400 MHz, DMSO, 298 K): δ 6.88–6.90 (dd, 1H, J = 8.8, 2.1 Hz, 6-indolinyl H's), 7.06 (s, 1H, 3-indolinyl H's), 7.33–7.38 (m, 1H, 5′-pyridyl H's), 7.46 (d, 1H, J = 2.1 Hz, 4-indolinyl H's), 7.63–7.69 (m, 1H, 7-indolinyl H's), 8.00 (t, 1H, J = 7.4 Hz, 4′-pyridyl H's), 8.06 (d, 1H, J = 7.4 Hz, 3′-pyridyl H's), 8.17 (s, 2H, phenyl H's), 8.22 (s, 2H, phenyl H's), 8.89 (d, 1H, J = 5.4 Hz, 6′-pyridyl H's). Positive-ion FAB-MS: m/z 1010.0 $[M]^+$; IR (KBr disc, ν/cm^{-1}): 2119, 2019 ν(N≡C); Elemental analyses Calcd (%) for **5**: C 32.10, H 1.20, N 5.55; found: C 32.30, H 1.34, N 5.58.

*4.4.6.6. [Rh(**Cl-pyind**)(CNC$_6$H$_2$Cl$_3$-2,4,6)$_2$] (**6**)* After recrystallization by the slow diffusion of diethylether vapor into a concentrated dichloromethane solution of **6**, analytically pure complex was obtained as yellowish green crystalline solids. Yield: 34.3%; ^{1}H NMR (400 MHz, $CDCl_3$, 298 K): δ 6.90 (s, 1H, 3-indolinyl H's), 6.94 (dd, 1H, J = 8.8, 1.7 Hz, 6-indolinyl H's), 7.02 (dd, 1H, J = 8.8, 5.6 Hz, 5′-pyridyl H's), 7.43 (s, 2H, phenyl H's), 7.46 (s, 2H, phenyl H's), 7.50 (d, 1H, J = 1.7 Hz, 4-indolinyl H's), 7.74–7.78 (m, 3H, 3′,4′-pyridyl H's, 7-indolinyl H's), 8.78 (d, 1H, J = 5.7 Hz, 6′-pyridyl H's); Positive-ion FAB-MS: m/z 743.7 $[M]^+$; IR (KBr disc, ν/cm^{-1}): 2119, 2027 ν(N≡C); Elemental analyses, Calcd (%) for **6**·0.5CH_2Cl_2: C 40.60, H 1.70, N 6.76; found: C 40.51, H 1.53, N 6.87.

*4.4.6.7. [Rh(**Cl$_2$pyind**)(CNC$_6$H$_2$Br-4-(CH$_3$)$_2$-2,6)$_2$] (**7**)* After recrystallization by the slow diffusion of diethylether vapor into a concentrated dichloromethane solution of **7**, analytically pure complex was obtained as yellow crystalline solids. Yield: 39.9%; ^{1}H NMR (400 MHz, $CDCl_3$, 298 K): δ 2.45 (s, 6H, $-CH_3$), 2.51 (s, 6H, $-CH_3$), 6.89 (d, 1H, J = 1.6 Hz, 3-indolinyl H's), 7.02 (m, 2H, 5′-pyridyl H's, 5-indolinyl H's), 7.29 (d, 4H, J = 5.5 Hz, phenyl H's), 7.54 (s, 1H, 7-indolinyl H's), 7.74 (td, 1H, J = 7.8, 1.4 Hz, 4′-pyridyl H's), 7.81 (d, 1H, J = 7.8 Hz, 3′-pyridyl H's), 8.60 (d, 1H, J = 5.4 Hz, 6′-pyridyl H's); Positive-ion FAB-MS: m/z 784.8 $[M]^+$; IR (KBr disc, ν/cm^{-1}): 2122, 2067 ν(N≡C); Elemental analyses Calcd (%) for **7**: C 47.42, H 2.95, N 7.14; found (%): C 47.38, H 3.19, N 7.10.

*4.4.6.8. [Rh(**Cl$_2$pyind**)(CNC$_6$H$_2$Cl$_2$-2,4-OCH$_3$-6)$_2$] (**8**)* After recrystallization by the slow diffusion of diethylether vapor into a concentrated acetone solution of **8**, analytically pure complex was obtained as yellow crystalline solids. Yield: 35.9%; ^{1}H NMR (400 MHz, DMSO, 298 K): δ 3.92 (s, 3H, $-OCH_3$), 3.97 (s, 3H, $-OCH_3$), 6.92 (d, 1H, J = 1.6 Hz, 3-indolinyl H's), 7.18 (d, 1H, J = 0.9 Hz, 5-indolinyl H's), 7.38–7.43 (m, 3H, 5′-pyridyl H's, phenyl H's), 7.45–7.49 (m, 2H, phenyl H's), 7.62 (dd, 1H, J = 1.6, 0.9 Hz, 7-indolinyl H's), 8.03 (td, 1H, J = 8.0, 1.6 Hz, 4′-pyridyl H's), 8.19 (d, 1H, J = 8.0 Hz, 3′-pyridyl H's), 8.82 (d, 1H, 6.1 Hz, 6′-pyridyl H's); Positive-ion FAB-MS: m/z 767.8 $[M]^+$; IR (KBr disc, ν/cm^{-1}): 2137, 2052 ν(N≡C); Elemental analyses Calcd (%) for **8**·0.5H_2O: C 44.76, H 2.33, N 7.20; found: C 44.62, H 2.47, N 6.95.

*4.4.6.9. [Rh(**Cl$_2$pyind**)(CNC$_6$H$_2$Br$_3$-2,4,6)$_2$] (**9**)* After recrystallization by the slow diffusion of diethylether vapor into a concentrated acetone solution of **9**, analytically pure complex was obtained as yellow crystalline solids. Yield: 36.4%; ^{1}H NMR (400 MHz, $CDCl_3$, 298 K): δ 6.91 (d, 1H, J = 1.7 Hz, 3-indolinyl H's), 7.01–7.06 (m, 2H, 5-indolinyl H's, 5′-pyridyl H's), 7.71–7.77 (m, 4H, 7-indolinyl H's, 4′-pyridyl and phenyl H's), 7.79–7.80 (m, 3H, 3′-pyridyl and phenyl H's), 8.83 (d, 1H, J = 5.4 Hz, 6′-pyridyl H's); Positive-ion FAB-MS: m/z 1045.0 $[M]^+$; IR (KBr disc, ν/cm^{-1}): 2111, 2016 ν(N≡C); Elemental analyses Calcd (%) for **9**·0.5$CH_3CH_2OCH_2CH_3$: C 32.20, H 1.49, N 5.18; found: C 32.18, H 1.37, N 5.37.

*4.4.6.10. [Rh(**Cl$_2$pyind**)(CNC$_6$H$_2$Cl$_3$-2,4,6)$_2$] (**10**)* After recrystallization by the slow diffusion of diethylether vapor into a concentrated acetone solution of **10**, analytically pure complex was obtained as

yellowish green crystalline solids. Yield: 42.7%; ^{1}H NMR (400 MHz, $CDCl_3$, 298 K): δ 6.93 (d, 1H, $J = 1.5$ Hz, 3-indolinyl H's), 7.01 (d, 1H, $J = 6.3$ Hz, 5-indolinyl H's), 7.06 (t, 1H, $J = 6.7$ Hz, 5′-pyridyl H's), 7.45 (s, 2H, phenyl H's), 7.47 (s, 2H, phenyl H's), 7.72 (s, 1H, 7-indolinyl H's), 7.75–7.78 (m, 2H, 3′,4′-pyridyl H's), 8.76 (d, 1H, $J = 4.9$ Hz, 6′-pyridyl H's); Positive-ion FAB-MS: m/z 778.0 $[M]^+$; IR (KBr disc, ν/cm^{-1}): 2111, 2001 ν(C≡N). Elemental analyses Calcd (%) for **10**·0.5CH_3COCH_3: C 42.42, H 1.75, N 6.94; found: C 42.14, H 2.05, N 6.96.

Acknowledgements

The work described in this paper was supported by grants from City University of Hong Kong (project nos. 7002435 and 7002594). W.-K. Chu and L.T.-L. Lo acknowledge the receipt of a Postgraduate Studentship from the City University of Hong Kong.

Appendix. Supplementary data

CCDC 819246–819248 contain the supplementary crystallographic data for **1,** [Rh(cod)(**Cl-pyind**)] and [Rh(cod)(**Cl$_2$pyind**)]. These data can be obtained free of charge via http://www.ccdc.cam.ac.uk/conts/retreving.html, or from the Cambridge Crystallographic Data Centre, 12 Union Road, Cambridge CB2 1EZ, UK; fax: +44 1223 336 033; or e-mail: deposit@ccdc.cam.ac.uk.

References

[1] Y. Chi, P.-T. Chou, Chem. Soc. Rev. 39 (2010) 638.
[2] P.-T. Chou, Y. Chi, Chem. Eur. J 13 (2007) 380.
[3] Y. Chi, P.-T. Chou, Chem. Soc. Rev. 36 (2007) 1421.
[4] J.A.G. Williams, A.J. Wilkinson, V.L. Whittle, Dalton Trans. (2008) 2081.
[5] M.S. Lowry, S. Bernhard, Chem. Eur. J 12 (2006) 7970.
[6] P.-T. Chou, Y. Chi, Eur. J. Inorg. Chem. (2006) 3319.
[7] Y. You, S.Y. Park, Dalton Trans. (2009) 1267.
[8] W.Y. Wong, C.L. Ho, J. Mater.Chem. 19 (2009) 4457.
[9] J.M. Patrick, A. White, H.M.I. Bruce, M.J. Beatson, D.S.C. Black, G.B. Deacon, N.C. Thomas, Dalton Trans. (1983) 2121.
[10] Q.-F. Zhang, K.-M. Cheung, I.D. Williams, W.-H. Leung, Eur. J. Inorg. Chem. (2005) 4780.
[11] E.Y. Li, Y.-M. Cheng, C.-C. Hsu, P.-T. Chou, G.-H. Lee, I.-H. Lin, Y. Chi, C.-S. Liu, Inorg. Chem. 45 (2006) 8041.
[12] K.-C. Hwang, J.-L. Chen, Y. Chi, C.-W. Lin, Y.-M. Cheng, G.-H. Lee, P.-T. Chou, S.-Y. Lin, C.-F. Shu, Inorg. Chem. 47 (2008) 3307.
[13] J.-K. Yu, Y.-H. Hu, Y.-M. Cheng, P.-T. Chou, S.-M. Peng, G.-H. Lee, A.J. Carty, Y.-L. Tung, S.-W. Lee, Y. Chi, C.-S. Liu, Chem. Eur. J. 10 (2004) 6255.
[14] Y.-M. Cheng, E.Y. Li, G.-H. Lee, P.-T. Chou, S.-Y. Lin, C.-F. Shu, K.-C. Hwang, Y.-L. Chen, Y.-H. Song, Y. Chi, Inorg. Chem. 46 (2007) 10276.
[15] M.G. Colombo, T.C. Brunold, T. Riedener, H.U. Güdel, M. Förtsch, H.-B. Bürgi, Inorg. Chem. 33 (1994) 545.
[16] V.V. Grushin, N. Herron, D.D. LeCloux, W.J. Marshall, V.A. Petrov, Y. Wang, Chem. Commun. (2001) 1494.
[17] S. Lamansky, P. Djurovich, D. Murphy, F. Abdel-Razzaq, R. Kwong, I. Tsyba, M. Bortz, B. Mui, R. Bau, M.E. Thompson, Inorg. Chem. 40 (2001) 1704.
[18] Y. Byun, W.S. Jeon, T.-W. Lee, Y.-Y. Lyu, S. Chang, O. Kwon, E. Han, H. Kim, M. Kim, H.-J. Lee, R.R. Das, Dalton Trans. (2008) 4732.
[19] L. Chassot, A.V. Zelewsky, Inorg. Chem. 26 (1987) 2814.
[20] J.-Y. Cho, K.Y. Suponitsky, J. Li, T.V. Timofeeva, S. Barlow, S.R. Marder, J. Organomet. Chem. 690 (2005) 4090.
[21] J. Brooks, Y. Babayan, S. Lamansky, P.I. Djurovich, I. Tsyba, R. Bau, M.E. Thompson, Inorg. Chem. 41 (2002) 3055.
[22] L.T.-L. Lo, C.-O. Ng, H. Feng, C.C. Ko, Organometallics 28 (2009) 3597.
[23] I. Ugi, U. Fetzer, U. Eholzer, H. Knupfer, K. Offermann, Angew. Chem., Int. Ed. Eng. 4 (1965) 472.
[24] W.P. Weber, G.W. Gokel, I.K. Ugi, Angew Chem., Int. Ed. Eng. 6 (1972) 530.
[25] R. Obrecht, R. Herrman, I. Ugi, Synthesis 4 (1985) 400.
[26] B. Janza, A. Studer, Org. Lett. 8 (2006) 1875.
[27] R.P. Thummel, V.J. Hegde, Org. Chem. 54 (1989) 1720.
[28] F. Wu, J. Hardesty, R.P. Thummel, J. Org. Chem. 63 (1998) 4055.
[29] F. Wu, C.M. Chamchoumis, R.P. Thummel, Inorg. Chem. 39 (2000) 584.
[30] Q. Liu, M.S. Mudadu, H. Schmider, R. Thummel, Y. Tao, S. Wang, Organometallics 21 (2002) 4743.
[31] S.T.H. Willems, P.H.M. Budzelaar, N.N.P. Moonen, R. de Gelder, J.M.M. Smits, A.W. Gal, Chem. Eur. J. 8 (2002) 1310.
[32] P.C. Wu, J.K. Yu, Y.H. Song, Y. Chi, P.T. Chou, S.M. Peng, G.H. Lee, Organometallics 22 (2003) 4938.
[33] F.C. Hsu, Y.L. Tung, Y. Chi, C.C. Hsu, Y.M. Cheng, M.L. Ho, P.T. Chou, S.M. Peng, A. Carty, Inorg. Chem. 45 (2006) 10188.
[34] J.J. Klappa, S.A. Geers, S.J. Schmidtke, L.A. MacManus-Spencer, K. McNeill, Dalton Trans. (2004) 883.
[35] D. Karshtedt, A.T. Bell, T.D. Tilley, Organometallics 25 (2006) 4471.
[36] B. Neumann, C. Krinninger, I.P. Lorenz, Eur. J. Inorg. Chem. (2007) 472.
[37] L. Yang, K.K. Cheung, A. Mayr, J. Organomet. Chem. 585 (1999) 26.
[38] C.C. Ko, L.T.L. Lo, C.O. Ng, S.M. Yiu, Chem. Eur. J. 16 (2010) 13773.
[39] C.O. Ng, L.T.L. Lo, S.M. Ng, C.C. Ko, N. Zhu, Inorg. Chem. 47 (2008) 7447.
[40] L. Weber, Angew. Chem. Int. Ed. 37 (1998) 1515.
[41] K.R. Mann, N.S. Lewis, R.M. Williams, H.B. Gray, J.G. Gordon II, Inorg. Chem. 17 (1978) 829.
[42] H. Isci, W.R. Mason, Inorg. Chem. 14 (1975) 913.
[43] G.L. Geoffroy, M.S. Wrighton, G.S. Hammond, H.B. Gray, J. Am. Chem. Soc. 96 (1974) 3105.
[44] K.R. Mann, J.G. Gordon II, H.B. Gray, J. Am. Chem. Soc. 97 (1975) 3553.
[45] A.L. Balch, J. Am. Chem. Soc. 98 (1976) 8049.
[46] V.M. Miskowski, S.F. Rice, H.B. Gray, J. Phys. Chem. 97 (1993) 4277.
[47] S.F. Rice, H.B. Gray, J. Am. Chem. Soc. 103 (1981) 1593.
[48] G.M. Sheldrick, SHELX-97, SHELX-97: Programs for Crystal Structure Analysis (Release 97–2) (1997).